ACS APPLIED MATERIALS & INTERFACES

Research Article

www.acsami.org

Strong, Self-Standing Oxygen Barrier Films from Nanocelluloses Modified with Regioselective Oxidative Treatments

Juho Antti Sirviö,*[,§] Aleksi Kolehmainen,[‡] Miikka Visanko,[†] Henrikki Liimatainen,[§] Jouko Niinimäki,[§] and Osmo E. O. Hormi[‡]

[†]Fibre and Particle Engineering Laboratory & Thule Institute, University of Oulu, P.O. Box 4300, FI-90014 Oulu, Finland

[‡]Department of Chemistry, University of Oulu, P.O. Box 3000, FI-90014 Oulu, Finland

[§]Fibre and Particle Engineering Laboratory, University of Oulu, P.O. Box 4300, FI-90014 Oulu, Finland

Supporting Information

ABSTRACT: In this work, three self-standing nanocellulose films were produced from birch pulp using regioselective oxidation and further derivatization treatments. The modified celluloses were synthesized using periodate oxidation, followed by chlorite oxidation, bisulfite addition, or reductive amination with amino acid taurine, which resulted in dicarboxylic acid cellulose (DCC), α-hydroxy sulfonic acid cellulose (HSAC), and taurine-modified cellulose (TC), respectively. The nanocelluloses were fabricated by mechanical disintegration using high-pressure homogenization. Mechanical and barrier properties of the nanocellulose films were characterized. Two (2,2,6,6-tetramethyl-piperidin-1-yl)oxyl (TEMPO) oxidation-based nanocellulose films were also produced, and their properties were compared to the periodate-based nanocellulose films. All of the periodate-based nanocellulose films showed high tensile strength (130−163 MPa) and modulus (19−22 GPa). Oxygen barrier properties of the films were superior to many synthetic and composite materials; in particular, the nanofibrillated DCC films had oxygen permeability as low as 0.12 cm^3 μm/(m^2 d kPa) at 50% relative humidity. Compared to films of TEMPO-oxidized nanocelluloses, all of the periodate-based nanocellulose films had similar or even better mechanical and barrier properties, demonstrating versatility of periodate oxidation to obtain nanocellulose films with adjustable properties. Also, for the first time, amino-acid-based cellulose modification was used in the production of nanocellulose.

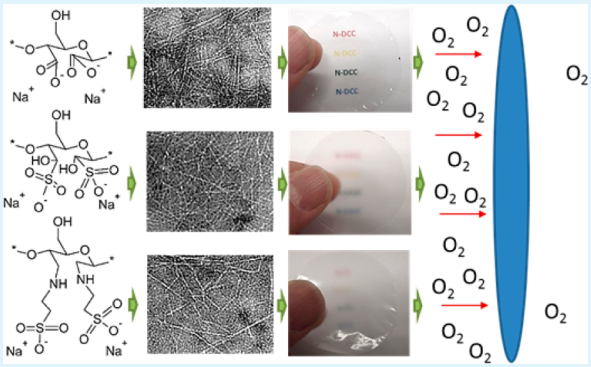

KEYWORDS: *regioselective oxidation, dialdehyde cellulose, nanocellulose, films, oxygen barrier, mechanical properties*

INTRODUCTION

Today, film materials with adjustable characteristics are highly desired. For example, films with high strength, good flexibility, and good barrier properties are required in packaging applications[1,2] and in electronic devices such as organic solar cells and organic light-emitting diodes (OLEDs).[3−6] Typically, these types of film materials are produced using oil-based synthetic polymers and composites of several different materials.

Nanocelluloses (also microfibrillated or nanofibrillated celluloses) are among the most promising resources to obtain novel products and also to replace many present oil-based materials. Nanocellulose can be produced using only purely mechanical methods.[7,8] However, chemical pretreatments can remarkably enhance the liberation of individual nanofibrils from cellulose matrix and reduce the energy consumption of production.[9] The most frequently investigated chemical pretreatments in nanocellulose production are (2,2,6,6-tetramethyl-piperidin-1-yl)oxyl (TEMPO) oxidation and carboxymethylation, both of which introduce an anionic charge on cellulose fibers, resulting in loosening of the hydrogen bond network of cellulose and increasing charge repulsion between cellulose fibrils.[10] These nanocelluloses have been studied as potential raw materials to obtain flexible and high-strength barrier films, especially in composite materials.[11,12]

One potential later approach to obtain nanocelluloses is regioselective periodate oxidation, which results in the formation of reactive dialdehyde cellulose (DAC). Readily attachable aldehyde groups enable the production of nanocelluloses with various functionalities.[13−16] In addition to nanocellulose production, periodate oxidation has been studied with fibrous and soluble celluloses to obtain several high-performing products such as chromatographic columns,[17] flocculation agents,[18,19] cross-linkers for collagen fibers,[20] and antimicrobial filter materials.[21]

Received: June 10, 2014
Accepted: August 4, 2014
Published: August 4, 2014

In the present work, the use of periodate-oxidized cellulose as a starting material for the self-standing nanocellulose films was studied. Three nanocellulose films with variable strength and barrier properties were fabricated. Periodate oxidation followed by chlorite oxidation, bisulfide addition, or reductive amination with taurine were used as modifying routes in nanocellulose production. Cellulose fibers and films were characterized using field-emission scanning electron microscopy (FESEM), transmission electron microscopy (TEM), wide-angle X-ray diffraction (WAXD), and ultraviolet−visible (UV-vis) spectrometry. Tensile mechanical properties and oxygen and water vapor barrier properties of the films were examined. For comparison, films from two TEMPO-oxidized nanocelluloses were also produced.

MATERIAL AND METHODS

Materials. Bleached birch pulp (*Betula pendula*) was obtained as dry sheets and used as a cellulose material after disintegration in deionized (DI) water. The properties of cellulose are presented elsewhere.[22]

All of chemicals used in periodate and TEMPO oxidations ($NaIO_4$, $C_9H_{18}NO$), further derivatizations (NaS_2O_5, $NH_2CH_2CH_2SO_3H$, $C_6H_7N{\cdot}BH_3$, $NaClO_2$ (purity of 80%) and CH_3COOH), and aldehyde and carboxyl content analyses ($NH_2OH{\cdot}HCl$, $CH_3COONa{\cdot}2H_2O$, NaCl, and NaOH) were obtained as p.a. grades from Sigma−Aldrich (Germany) and were used without further purification. DI water was used throughout the experiments, except during the preparation of TEM samples, where ultrapure water (ISO 3696) was used.

Synthesis of Cellulose Derivatives. Two-step reactions were used to fabricate periodate-based celluloses. At first, cellulose pulp was oxidized with periodate as previously described.[23] In brief, 9.00 g of cellulose was oxidized using 7.38 g of sodium periodate at 55 °C for 3 h in the absence of light. DAC with an aldehyde content of 1.68 mmol/g was obtained (i.e., 14% of the cellulose AGUs were oxidized). The product was stored at 4 °C in a nondried state.

Dicarboxylic acid cellulose (DCC) was prepared as reported earlier.[14] In brief, 4.50 g of nondried DAC was reacted with 4.53 g of sodium chlorite in a 1 M aqueous solution of acetic acid for 48 h at room temperature.

α-Hydroxy sulfonic acid cellulose (HSAC) was prepared as described in our previous study.[15] In brief, 2.00 g of nondried DAC was allowed to react with 3.20 g of sodium metabisulfite for 72 h at room temperature.

Taurine cellulose (TC) was prepared as described previously.[24] In brief, 4.00 g of nondried DAC was allowed to react with 8.40 g of taurine at pH 4.5 using 1.44 g of 2-picoline borane as a reductant. The reaction was allowed to proceed for 72 h at room temperature.

Two TEMPO-oxidized celluloses were prepared using a slightly modified method that has been reported in the literature. In first method,[25] 3.00 g of cellulose was dispersed into 270 mL of phosphate buffer (0.05 M, pH 6.8) in flask; then, 0.048 g of TEMPO was added followed by sequential addition of 4.69 mL NaClO solution (contained 2.24 mL of 1.34 M NaClO solution in same phosphate buffer as used in cellulose dispersion) and 3.39 g of $NaClO_2$ (80%). Flask was equipped with reflux condenser and reaction was continued under mixing for 24 h at 60 °C. The obtained product was designated as TOC1.

In the second TEMPO oxidation method,[26] 5.00 g of cellulose was added to water solution (375 mL) containing 0.0625 g of TEMPO and 0.625 NaBr. To this suspension, 23.5 mL of 1.34 M NaClO solution was added and the reaction solution was mixed at room temperature, maintaining the pH at 10.5, using 0.5 M NaOH solution. After the decrease of pH ceased, pH was adjusted to 7, using 0.5 M HCl solution. The obtained product was designated as TOC2. All of the cellulose derivatives were filtrated, washed with DI water, and stored at 4 °C in a nondried state.

The aldehyde content of DAC was determined by the method described previously.[23] The carboxylic acid contents of DCC, TOC1, TOC2, and α-hydroxy sulfonic acid content of HSAC were determined via conductometric titration using a procedure described in the literature.[27,28] The taurine group content of TC was determined using an elemental analyzer (Flash 2000 CHNS/O, Thermo Scientific) by analyzing the nitrogen content of the dried sample.

Preparation of Nanocelluloses. Nanofibrillation of modified celluloses was performed using a two-chamber high-pressure homogenizer (APV-2000, Denmark). Prior to the homogenizing, pH of the nonfibrillated cellulose suspensions (0.5%) was adjusted to ∼7.5 using a dilute NaOH solution. For TC suspension, pH was adjusted to ∼10. The suspensions were then passed three times through the homogenizer at pressures of 250, 500, and 570 bar to form nanocellulose suspensions. To prevent clogging, the TC and TOC1 suspensions were first passed through the homogenizer with a pressure of 100 bar, after which they were homogenized with pressures of 250, 500, and 570 bar.

Preparation of Nanocellulose Films. The nanocellulose films were prepared using a solvent-casting method. 606 mL of the nanocellulose dispersion (0.25%) was mixed for 1 min at 11 000 rpm with an Ultra Turrax mixer (Germany) degassed and cast in a polystyrene tray with an area of 505 cm^2, resulting in films with a grammage of 30 g/m^2. Films were allowed to dry for 5 days in an air-ventilated cabinet at room temperature. Drying was monitored visually.

Mechanical Properties. The films were cut into 15 mm × 150 mm strips and conditioned at 23 °C and 50% relative humidity (50% RH) for 48 h before testing, and all the tests were also performed under these conditions. The specific tensile strength (σ/ρ), elongation at break, and specific modulus (E/ρ) were determined using ISO Standard 527-3 and a Lorentzen & Wettre strength tester (Sweden). A test speed of 50 mm/min was used. Initial distance between grips was set to 100 mm. Tensile strength (σ) and modulus (E) was calculated using the density (ρ) from σ/ρ and E/ρ, respectively. For all of the samples, five test specimen were measured and results are presented as an average of these results.

Film thicknesses were determined as the averages of five random positions of the film using a Lorentzen & Wettre thickness meter (Sweden).

Field-Emission Scanning Electron Microscopy. Field-emission scanning electron microscopy (FESEM) (Zeiss Ultra Plus, Carl Zeiss SMT AG, Germany) was used to examine the morphology of cellulose pulp and the chemically modified cellulose fibers. Fibers were sputter-coated with Pd, and an accelerating voltage of 5 kV was used.

Transmission Electron Microscopy. The morphological features of the fabricated nanocelluloses were analyzed with a Tecnai G2 Spirit transmission electron microscopy (TEM) system (FEI Europe, Eindhoven, The Netherlands). Samples were prepared by diluting each sample with ultrapure water. A small droplet of the dilution was dosed on top of a carbon-

Scheme 1. (a) Periodate Oxidation of Cellulose, and Further Derivatization of DAC by (b) Chloride Oxidation, (c) Bisulfide Addition, (d) Reductive Amination with Taurine, and (e) TEMPO Oxidation of Cellulose

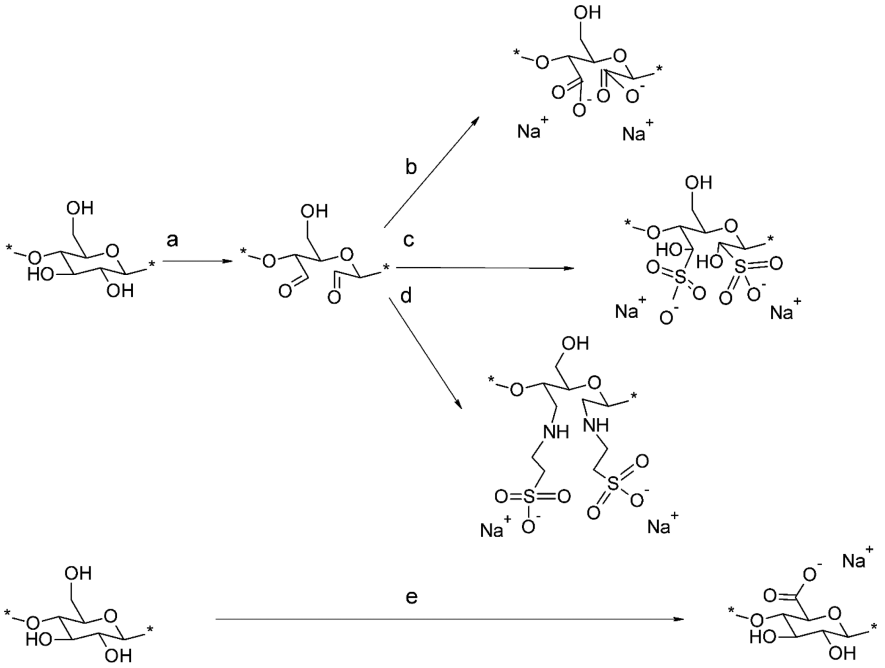

coated and glow-discharged copper grid. Excess amounts of the sample were removed from the grid by touching the droplet with a corner of a filter paper. Negative staining of the samples was performed by placing a droplet of uranyl acetate (2% w/v) on top of each specimen. The excess amount of the uranyl acetate was removed with filter paper as described above. Grids were dried at room temperature and analyzed at 100 kV under standard conditions. Images were captured by Quemesa CCD camera and iTEM image analysis software (Olympus Soft Imaging Solutions GmbH, Munster, Germany) was used to measure individual nanocelluloses width. A total of 50 fibrils of each nanocellulose grade were measured. The final results were averaged and standard deviations were calculated.

X-ray Diffraction. The crystalline structure of the cellulose after chemical modifications and nanofibrillation was investigated using wide-angle X-ray diffraction (WAXD). Measurements were conducted on a Siemens D5000 diffractometer equipped with a Cu Kα radiation source (k = 0.1542 nm). Samples were prepared by pressing tablets of freeze-dried cellulose to a thickness of 1 mm. Scans were taken over a 2θ (Bragg angle) range from 5° to 50° at a scanning speed of 0.02°/s, using a step time of 1 s. The degree of crystallinity, in terms of the crystallinity index (CrI), was calculated from the peak intensity of the main crystalline plane (002) diffraction (I_{002}) at 22.2° and from the peak intensity at 18.0° associated with the amorphous fraction of cellulose (I_{am}), according to the following equation:

$$\mathrm{CrI}\ (\%) = \left(\frac{I_{002} - I_{am}}{I_{002}}\right) \times 100$$

Optical Transmittance. The transmittance of 0.1% nanocellulose suspensions and the nanocellulose films was measured at wavelengths of 300−800 nm using UV−vis spectroscopy (Shimadzu, Japan). The transmittance of the nanocellulose films was measured by inserting a slide of each film in the cuvette stand, so that the beam was oriented at 90°, with respect to the slide.

Water Vapor Permeability. Water vapor permeability (WVP) was determined using ASTM Standard E 96-95. All films (three sample per film) were conditioned at 23 °C and 50% RH for 48 h before testing. About one-fourth of a 100-mL Schott Duran laboratory glass bottle was filled with deionized water and the test specimen was placed between a bottle and an open-end-cap. Rubber seal was used to ensure tight sealing. The test assembly was weighted and placed in a controlled condition chamber (23 °C and 50% RH, equipped with a fan to ensure good circulation of air inside the chamber) and the weight lost was recorded at regular intervals for 8 h. The steady state was reached during the first day and the weight loss over the subsequent four days was calculated. Slope of the strain line was calculated from the weight loss versus time and water vapor transmission rate (WVTR) was calculated by dividing the slope by the exposed film area. The WVP value was calculated as follows:

$$\mathrm{WVP} = \frac{\mathrm{WVTR}}{S(R_1 - R_2)}$$

where S is the saturation vapor pressure at the test temperature (28−102 Pa at 23 °C), R1 is the relative humidity in the dish expressed as a fraction (1), and R_2 is the relative humidity at the vapor sink expressed as a fraction (0.5).

Oxygen Transmission Rate and Permeability. The oxygen gas transmission rate (OTR) of the films was measured using an oxygen permeability (OP) analyzer with a coulometric sensor (Model M8001, Systech Illinois, Oxfordshire, U.K.). The film was exposed to 100% oxygen on one side and oxygen-free nitrogen on the other side. The OP was calculated by multiplying the OTR by the thickness of the film and dividing it by the oxygen gas partial pressure difference between the two sides of the film. The measurements were carried out at 23 °C, normal atmospheric pressure, and 50% RH. The specimen area

was 5 cm^2, and the thickness of the film was measured before analysis at five points with a micrometer at 1 μm precision. The OP was determined in duplicate.

RESULTS AND DISCUSSION

Synthesis of Cellulose Derivatives and Their Nanofibrillation. To produce the nanocellulose films with adjustable properties, three periodate-based nanocelluloses were fabricated. Two of the methods, i.e., routes for DCC and HSAC have been previously reported.[14,15] The anionic charges of DCC and HSAC were 1.75 and 0.51 mmol/g, respectively. In the third method, periodate-oxidized cellulose was first derivatized via reductive amination using amino acid taurine. The taurine group content of TC was determined to be 0.75 mmol/g. TEMPO-oxidized celluloses TOC1 and TOC2 possessed anionic charges of 0.5 and 1.28 mmol/g, respectively. These values are slightly lower than those reported in the literature.[25,26] Differences may arise from the use of different cellulose sources. The chemical modifications of cellulose used in this study are presented in Scheme 1.

FESEM images of chemically modified cellulose fibers are presented in the Supporting Information (Figure S1). After periodate oxidation, the morphology of cellulose fibers is mostly unchanged. However, after further derivatizations of DAC, and after TEMPO oxidations, fibers were slightly translucent, indicating that a chemical modification slightly alters the fiber structure of cellulose. Compared to other modified celluloses, TOC2 fibers were shorter, slightly fibrillated, and exhibited a ballooning-like structure, which is an indication that TEMPO oxidation under alkaline conditions caused a greater amount of spontaneous fibrillation than other chemical modifications.

A high-pressure homogenizer was used in fabrication of nanocelluloses from the cellulose derivatives. Because of the presence of a secondary amine group in TC, the pH of the TC suspension was adjusted to 10 before nanofibrillation, to ensure sufficiently high surface charge density. Other celluloses were fibrillated at pH 7. All of the suspensions passed through the homogenizer without clogging, and viscous and transparent gels were obtained.

In the range of 400−800 nm, all the nanocellulose suspensions (0.1%) had optical transmittance of ∼70% or higher, indicating that all cellulose were successfully disintegrated to nanofibrils (see Figure 1). Both highly charged nanocelluloses, N-DCC and N-TOC2, had very high transparency (∼88% at 600 nm).

X-ray diffractograms of the cellulose derivatives after nanofibrillation are presented in Figure 2a. All of the celluloses showed characteristic peaks of cellulose I, with main 2θ diffraction angles close to 14.5°, 16.0°, and 22.2° associated with the 101, 10$\bar{1}$, and 002 crystalline planes, respectively. This indicates that no rearrangement of the cellulose structure into another crystalline form occurred. However, as the peaks of different cellulose crystalline structures are close to each other, higher resolution study should be performed to identify the presence of other crystalline structures.

The CrI values of cellulose and its derivatives before and after nanofibrillation are presented in Figure 2b. DAC exhibited the lowest CrI value, compared to other derivatives. It is known that periodate oxidation can decrease the crystallinity of cellulose as periodate also modifies the cellulose molecules inside cellulose crystals.[29] On the other hand, TEMPO oxidation mainly modifies amorphous parts and surfaces of

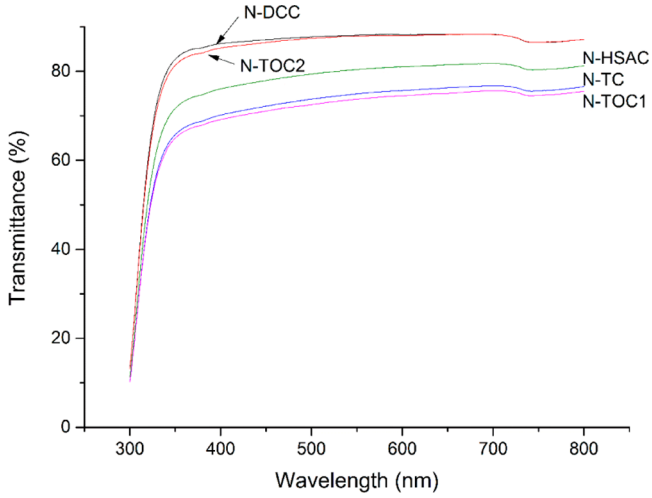

Figure 1. Optical transmittance of the 0.1% nanocellulose solutions.

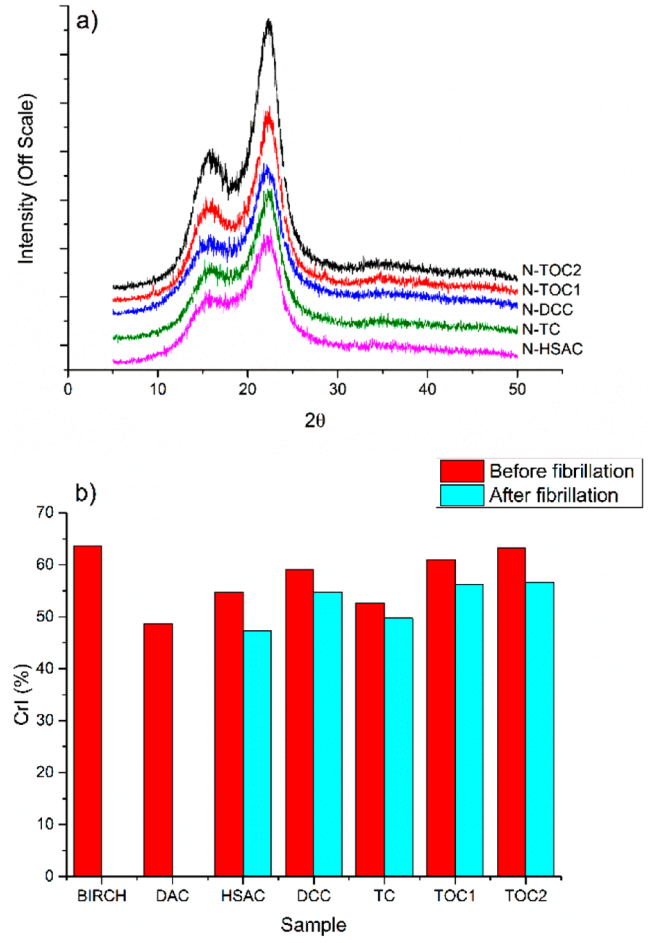

Figure 2. (a) Diffractograms of nanocelluloses, and (b) calculated crystallinity index (CrI) values of cellulose and its derivatives before and after fibrillation.

cellulose crystals.[30] Slightly higher CrI values for HSAC, DCC, and TC, compared to that for DAC, is most likely due to partial dissolution of the amorphous part of DAC during the sequential chemical treatment.

After nanofibrillation, all of the derivatives showed small decreases in their CrI, e.g., N-HSAC had a CrI value that was 15.6% lower than that for HSAC, while the CrI value of DCC

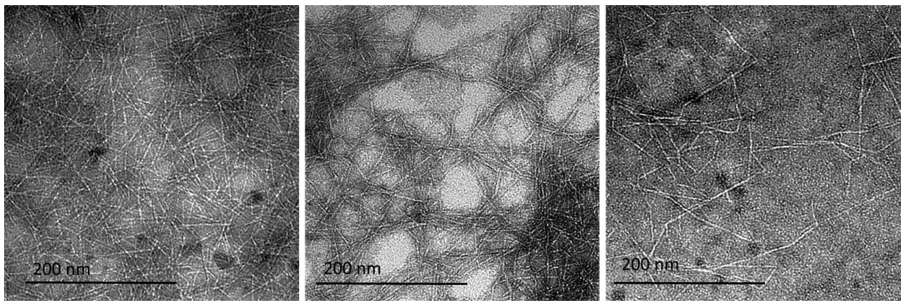

Figure 3. TEM images of periodate-based nanocelluloses: (left) N-HSAC, (middle) N-DCC, and (right) N-TC.

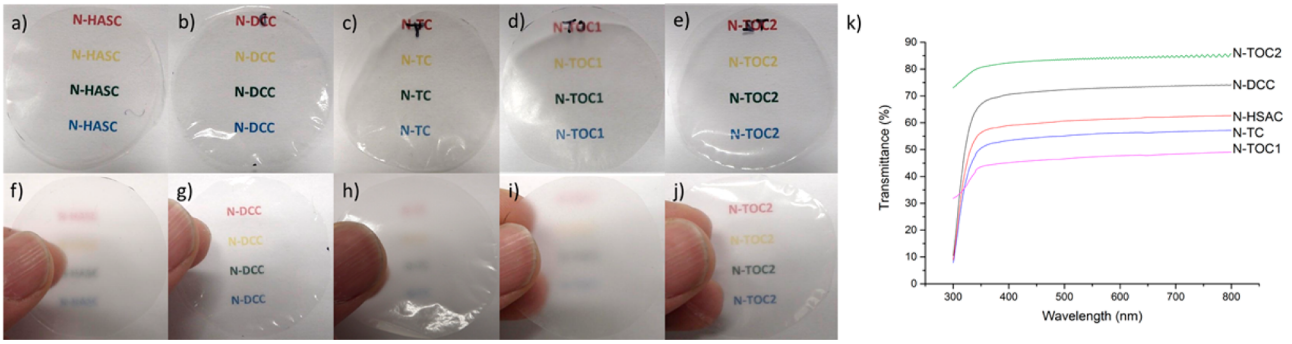

Figure 4. Optical properties of the nanocellulose films. Films were placed directly on top of the background image ((a) N-HSAC, (b) N-DCC, (c) N-TC, (d) N-TOC1, and (e) N-TOC2) and held a few centimeters above the background image ((f) N-HSAC, (g) N-DCC, (h) N-TC, (i) N-TOC1, and (j) N-TOC2). Panel k shows the transmittance of the nanocellulose films.

Table 1. OTR, OP, and WVP Values of Nanocellulose Films[a]

film	OTR[b] ($cm^3/(m^2\ d)$)	OP[b] ($cm^3\ \mu m/(m^2\ d\ kPa)$)	WVP ($g/(Pa\ s\ m^2)$)
N-HASC	0.74 ± 0.00	0.20 ± 0.00	$7.5 \times 10^{-7} \pm 1.7 \times 10^{-8}$
N-DCC	0.42 ± 0.03	0.12 ± 0.05	$7.3 \times 10^{-7} \pm 2.3 \times 10^{-8}$
N-TC	1.32 ± 0.04	0.44 ± 0.07	$7.2 \times 10^{-7} \pm 2.9 \times 10^{-8}$
N-TOC1	0.56 ± 0.01	0.18 ± 0.02	$7.3 \times 10^{-7} \pm 4.0 \times 10^{-9}$
N-TOC2	1.80 ± 0.02	0.38 ± 0.04	$7.8 \times 10^{-7} \pm 6.1 \times 10^{-9}$

[a]The data correspond to the mean ± standard deviation (SD) of two measurements for OTR and OP and three measurements for WVP. [b]At 23 °C, 50% RH.

decreased only 8% during the nanofibrillation. The decrease in CrI during the nanofibrillation is attributed to strong shear forces of the homogenization, which may loosen the crystalline structure and result in peeling of the cellulose chains on the crystallites.[31]

Typical TEM images of periodate-based nanocelluloses are presented in Figure 3 (images of TEMPO-oxidized nanocellulose are presented in Figure S2 in the Supporting Information). These images confirmed the efficient nanofibrillation of cellulose during the homogenization. Average widths of N-HSAC, N-DCC, N-TC, N-TOC1, and N-TOC2 were 3.8 ± 0.8, 3.1 ± 0.5, 2.9 ± 0.6, 3.2 ± 0.6 and 5.5 ± 0.6 nm, confirming that all of the chemical modifications result in liberation of individual nanofibrils after high-pressure homogenization. Results are inconsist with studies reported in the literature of TEMPO-oxidized nanocelluloses.[25,32]

Nanocellulose Films. Nanocellulose films were prepared using a solvent-casting method. After drying for 5 days, all of the films could easily peeled off from supporting polystyrene trays. Strong self-standing films were obtained, because all of the films were flexible and could be easily handled.

UV-vis Spectroscopy. For the devices such as OLEDs and solar cells, film materials with high transparency are required. All of the nanocellulose films exhibited very high transparency and had transmittance over 50% at visible spectrum, except the N-TOC1 film, which had a transmittance of ~45% in the visible spectrum (Figure 4k). The all of the films appeared highly transparent, which could be seen when placed on the top of the background image (see Figures 4a–e). However, when N-HSAC, N-TC, and N-TOC1 were held a few centimeters above the background image, it appeared hazy (see Figures 4f, 4h, and 4i, whereas when N-DCC or N-TOC2 were involved, the images were still clearly visible (see Figures 4g and 4j). The haziness of the background image indicated large light scattering in the film structure.

Oxygen Transmission Rate and Permeability. High oxygen barrier properties are crucial for many applications. For instance, electronic devices may suffer disastrous malfunctions because of the penetration of oxygen through their protection/supporting layers.[33] Nanocellulose films have been shown to possess very high oxygen barrier properties, especially in the form of nanocomposites, in which they are mixed with inorganic (nano)particles. Our results presented in Table 1 show that, at 50% RH, the periodate-based nanocellulose films exhibit very low OP values and their oxygen barrier properties can be varied by choosing suitable sequential derivatization. OP

Table 2. Thickness, Density, and Mechanical Properties of the Nanocellulose Films[a]

film	thickness (μm)	specific strength (kNm/kg)	strength (MPa)	strain (%)	specific modulus (MN m/kg)	modulus (GPa)	density (g/cm^3)
N-HSAC	28	152.0 ± 1.5	162.9 ± 2.1	1.6 ± 0.2	19.7 ± 0.2	21.1 ± 0.2	1.07
N-DCC	29	134.6 ± 0.8	139.2 ± 1.2	1.2 ± 0.1	21.7 ± 0.3	22.4 ± 0.4	1.03
N-TC	34	147.9 ± 7.0	130.5 ± 7.7	1.5 ± 0.3	21.8 ± 0.4	19.3 ± 0.5	0.88
N-TOC1	35	129.8 ± 6.9	118.0 ± 12.2	0.6 ± 0.1	33.4 ± 0.6	30.3 ± 1.0	0.91
N-TOC2	22	89.0 ± 10.7	121.3 ± 18.8	0.7 ± 0.1	22.0 ± 0.3	30.0 ± 0.5	1.36

[a]The data correspond to the mean ± SD of five measurements.

value of N-DCC film was as low as 0.12 cm^3 μm/(m^2 d kPa). This is comparable to the oxygen barrier properties of the nanocellulose-nanoclay composite films reported earlier, and this value represents one of the lowest OP values reported to the noncomposite biobased materials.[34] In addition, the OP value of N-DCC film is significantly lower than OP values of many synthetic materials, such as polypropylene (500−1000 cm^3 μm/(m^2 d kPa)) and poly(vinyl chloride) (20−80 cm^3 μm/(m^2 d kPa)) at 50% RH and is even comparable to OP values of some high oxygen barrier polymers, such as poly(vinyl alcohol) (0.2 cm^3 μm/(m^2 d kPa)) and poly(vinylidene chloride) (0.1−0.3 cm^3 μm/(m^2 d kPa)) at 0% RH.[35] N-HSAC and N-TOC1 films also exhibit very low OP, close to N-DCC film, whereas N-TC and N-TOC2 films had OP values ∼3-fold higher than those for N-DCC, H-HASC, and N-TOC1 films.

Water Vapor Permeability. Since cellulose is a highly hydrophilic material, cellulose-based films usually have low water vapor barrier properties, especially when compared to synthetic oil-based materials.[36] As shown in Table 1, all of the nanocellulose films exhibit similar WVP, which may indicate that they have quite similar hydrophilicity. In the literature, the water vapor barrier properties of cellulose-based films have been improved by inorganic particles or by coating with hydrophobic materials.[37,38] Therefore, it is most likely that the water barrier properties of periodate-based nanocellulose films can also be improved using the aforementioned methods.

Mechanical Properties. Tensile strength of periodate-based nanocellulose films were in the range of 130−162 MPa (Table 2). Compared to films produced from nonfibrillated DCC, HSAC, and TC, these results are more than three magnitudes higher.[24] On the other hand, strain values are significantly lower, especially for N-DCC and N-TC films, compared to films produced from nonfibrillated materials. Because of the significantly higher surface area, nanocellulose produces films with a denser hydrogen bond network than their nonfibrillated counterparts, resulting in the formation of films with higher mechanical properties. Tensile strength of periodate-based nanocellulose films are also higher than those of commercially available cellulose-based materials such as cellophane (50−120 MPa)[39] and cellulose acetate (56.2 MPa).[40]

Compared to TEMPO-oxidized nanocellulose films, periodate-based nanocellulose films had higher strength values; specific tensile strengths were especially higher (4%−70%). On the other hand, the N-TOC1 and N-TOC2 films were significantly stiffer than the periodate-based nanocellulose films, having modulus values that were ∼10 GPa higher. However, all of the nanocellulose films exhibited similar specific modulus values, except the N-TOC1 film, which had a specific modulus value that was ∼10 GPa higher than that for the other films. TEMPO-based nanocellulose films had ∼2-fold lower elongation at break values than periodate-based films.

CONCLUSIONS

Regioselective periodate oxidation, followed by sequential chemical treatments, was demonstrated to be a versatile method to obtain self-standing nanocellulose films with adjustable properties. The nanocellulose film with very high tensile strength can be obtained via bisulfide addition treatment of DAC. On the other hand, the N-DCC film had remarkably low oxygen permeability, which is among the lowest obtained from single component biomaterials and comparable with the nanocellulose-based composites. In addition, the potential use of natural amino acids in the fabrication of nanocellulose with properties similar to more traditional nanocelluloses was demonstrated.

ASSOCIATED CONTENT

Supporting Information

The FESEM images of chemically modified cellulose fibers and TEM images of TEMPO-oxidized nanocellulose are included in the Supporting Information. This material is available free of charge via the Internet at http://pubs.acs.org.

AUTHOR INFORMATION

Corresponding Author

*Tel.: +358 2944 824 24. Fax: +358 855 323 27. E-mail: Juho.Sirvio@oulu.fi.

Author Contributions

The manuscript was written through contributions from all of the authors. All authors have given approval to the final version of the manuscript.

Notes

The authors declare no competing financial interest.

ACKNOWLEDGMENTS

Dr. Kirsi Mikkonen is gratefully acknowledged for oxygen barrier measurements.

REFERENCES

(1) Miller, K. S.; Krochta, J. M. Oxygen and aroma Barrier Properties of Edible Films: A Review. *Trends Food Sci. Technol.* **1997**, *8*, 228−237.
(2) Duncan, T. V. Applications of Nanotechnology in Food Packaging and Food Safety: Barrier Materials, Antimicrobials and Sensors. *J. Colloid Interface Sci.* **2011**, *363*, 1−24.
(3) Krebs, F. C.; Gevorgyan, S. A.; Alstrup, J. A Roll-to-Roll Process to Flexible Polymer Solar Cells: Model Studies, Manufacture and Operational Stability Studies. *J. Mater. Chem.* **2009**, *19*, 5442.
(4) Charton, C.; Schiller, N.; Fahland, M.; Holländer, A.; Wedel, A.; Noller, K. Development of High Barrier Films on Flexible Polymer Substrates. *Thin Solid Films* **2006**, *502*, 99−103.
(5) Okahisa, Y.; Yoshida, A.; Miyaguchi, S.; Yano, H. Optically Transparent Wood−Cellulose Nanocomposite as a Base Substrate for Flexible Organic Light-Emitting Diode Displays. *Compos. Sci. Technol.* **2009**, *69*, 1958−1961.

(6) Hu, L.; Zheng, G.; Yao, J.; Liu, N.; Weil, B.; Eskilsson, M.; Karabulut, E.; Ruan, Z.; Fan, S.; Bloking, J. T.; McGehee, M. D.; Wågberg, L.; Cui, Y. Transparent and Conductive Paper from Nanocellulose Fibers. *Energy Environ. Sci.* **2013**, *6*, 513−518.
(7) Herrick, F. W.; Casebier, R. L.; Hamilton, J. K.; Sandberg, K. R. Microfibrillated Cellulose: Morphology and Accessibility. *J. Appl. Polym. Sci.: Appl. Polym. Symp.* **1983**, *37*, 797−813.
(8) Taniguchi, T.; Okamura, K. New Films Produced from Microfibrillated Natural Fibres. *Polym. Int.* **1998**, *47*, 291−294.
(9) Abdul Khalil, H. P. S.; Davoudpour, Y.; Islam, M. N.; Mustapha, A.; Sudesh, K.; Dungani, R.; Jawaid, M. Production and Modification of Nanofibrillated Cellulose Using Various Mechanical Processes: A Review. *Carbohydr. Polym.* **2014**, *99*, 649−665.
(10) Wågberg, L.; Decher, G.; Norgren, M.; Lindström, T.; Ankerfors, M.; Axnäs, K. The Build-Up of Polyelectrolyte Multilayers of Microfibrillated Cellulose and Cationic Polyelectrolytes. *Langmuir* **2008**, *24*, 784−795.
(11) Wu, C.-N.; Saito, T.; Fujisawa, S.; Fukuzumi, H.; Isogai, A. Ultrastrong and High Gas-Barrier Nanocellulose/Clay-Layered Composites. *Biomacromolecules* **2012**, *13*, 1927−1932.
(12) Ho, T. T. T.; Zimmermann, T.; Ohr, S.; Caseri, W. R. Composites of Cationic Nanofibrillated Cellulose and Layered Silicates: Water Vapor Barrier and Mechanical Properties. *ACS Appl. Mater. Interfaces* **2012**, *4*, 4832−4840.
(13) Tejado, A.; Alam, M. N.; Antal, M.; Yang, H.; van de Ven, T. G. M. Energy Requirements for the Disintegration of Cellulose Fibers into Cellulose Nanofibers. *Cellulose* **2012**, *19*, 831−842.
(14) Liimatainen, H.; Visanko, M.; Sirviö, J. A.; Hormi, O. E. O.; Niinimaki, J. Enhancement of the Nanofibrillation of Wood Cellulose through Sequential Periodate−Chlorite Oxidation. *Biomacromolecules* **2012**, *13*, 1592−1597.
(15) Liimatainen, H.; Visanko, M.; Sirviö, J.; Hormi, O.; Niinimäki, J. Sulfonated Cellulose Nanofibrils Obtained from Wood Pulp Through Regioselective Oxidative Bisulfite Pre-treatment. *Cellulose* **2013**, *20*, 741−749.
(16) Liimatainen, H.; Suopajärvi, T.; Sirviö, J.; Hormi, O.; Niinimäki, J. Fabrication of Cationic Cellulosic Nanofibrils Through Aqueous Quaternization Pretreatment and Their Use in Colloid Aggregation. *Carbohydr. Polym.* **2014**, *103*, 187−192.
(17) Kim, U.-J.; Kuga, S. Reactive Interaction of Aromatic Amines with Dialdehyde Cellulose Gel. *Cellulose* **2000**, *7*, 287−297.
(18) Liimatainen, H.; Sirviö, J.; Sundman, O.; Visanko, M.; Hormi, O.; Niinimäki, J. Flocculation Performance of a Cationic Biopolymer Derived from a Cellulosic Source in Mild Aqueous Solution. *Bioresour. Technol.* **2011**, *102*, 9626−9632.
(19) Liimatainen, H.; Sirviö, J.; Sundman, O.; Hormi, O.; Niinimäki, J. Use of Nanoparticular and Soluble Anionic Celluloses in Coagulation-Flocculation Treatment of Kaolin Suspension. *Water Res.* **2012**, *46*, 2159−2166.
(20) Kanth, S. V.; Ramaraj, A.; Rao, J. R.; Nair, B. U. Stabilization of Type I Collagen Using Dialdehyde Cellulose. *Process Biochem.* **2009**, *44*, 869−874.
(21) Woo, M.-H.; Lee, J.-H.; Rho, S.-G.; Ulmer, K.; Welch, J. C.; Wu, C.-Y.; Song, L.; Baney, R. H. Evaluation of the Performance of Dialdehyde Cellulose Filters against Airborne and Waterborne Bacteria and Viruses. *Ind. Eng. Chem. Res.* **2011**, *50*, 11636−11643.
(22) Liimatainen, H.; Sirviö, J.; Haapala, A.; Hormi, O.; Niinimäki, J. Characterization of Highly Accessible Cellulose Microfibers Generated by Wet Stirred Media Milling. *Carbohydr. Polym.* **2011**, *83*, 2005−2010.
(23) Sirvio, J.; Hyvakko, U.; Liimatainen, H.; Niinimaki, J.; Hormi, O. Periodate Oxidation of Cellulose at Elevated Temperatures Using Metal Salts as Cellulose Activators. *Carbohydr. Polym.* **2011**, *83*, 1293−1297.
(24) Sirviö, J. A.; Liimatainen, H.; Niinimäki, J.; Hormi, O. Sustainable Packaging Materials Based on Wood Cellulose. *RSC Adv.* **2013**, *3*, 16590−16596.
(25) Song, J.; Tang, A.; Liu, T.; Wang, J. Fast and Continuous Preparation of High Polymerization Degree Cellulose Nanofibrils and Their Three-Dimensional Macroporous Scaffold Fabrication. *Nanoscale* **2013**, *5*, 2482−2490.
(26) Saito, T.; Nishiyama, Y.; Putaux, J.-L.; Vignon, M.; Isogai, A. Homogeneous Suspensions of Individualized Microfibrils from TEMPO-Catalyzed Oxidation of Native Cellulose. *Biomacromolecules* **2006**, *7*, 1687−1691.
(27) Katz, S.; Beatson, R. P.; Scallan, A. M. The Determination of Strong and Weak Acidic Groups in Sulfite Pulps. *Sven. Papperstidn.* **1984**, *87*, 48−53.
(28) Rattaz, A.; Mishra, S. P.; Chabot, B.; Daneault, C. Cellulose Nanofibres by Sonocatalysed-TEMPO-Oxidation. *Cellulose* **2011**, *18*, 585−593.
(29) Varma, A. J.; Jamdade, Y. K.; Nadkarni, V. M. Wide-Angle X-ray Diffraction Study of the Effect of Periodate Oxidation and Thermal Treatment on the Structure of Cellulose Powder. *Polym. Degrad. Stab.* **1985**, *13*, 91−98.
(30) Saito, T.; Isogai, A. TEMPO-Mediated Oxidation of Native Cellulose. The Effect of Oxidation Conditions on Chemical and Crystal Structures of the Water-Insoluble Fractions. *Biomacromolecules* **2004**, *5*, 1983−1989.
(31) Besbes, I.; Alila, S.; Boufi, S. Nanofibrillated Cellulose from TEMPO-Oxidized Eucalyptus Fibres: Effect of the Carboxyl Content. *Carbohydr. Polym.* **2011**, *84*, 975−983.
(32) Saito, T.; Kimura, S.; Nishiyama, Y.; Isogai, A. Cellulose Nanofibers Prepared by TEMPO-Mediated Oxidation of Native Cellulose. *Biomacromolecules* **2007**, *8*, 2485−2491.
(33) Chang, Y.-F.; Ji, L.; Wu, Z.-J.; Zhou, F.; Wang, Y.; Xue, F.; Fowler, B.; Yu, E. T.; Ho, P. S.; Lee, J. C. Oxygen-Induced Bi-Modal Failure Phenomenon in SiO_x-Based Resistive Switching Memory. *Appl. Phys. Lett.* **2013**, *103*, 033521.
(34) Aulin, C.; Salazar-Alvarez, G.; Lindström, T. High Strength, Flexible and Transparent Nanofibrillated Cellulose−Nanoclay Biohybrid Films with Tunable Oxygen and Water Vapor Permeability. *Nanoscale* **2012**, *4*, 6622.
(35) Lange, J.; Wyser, Y. Recent Innovations in Barrier Technologies for Plastic Packaging—A Review. *Packag. Technol. Sci.* **2003**, *16*, 149−158.
(36) Findenig, G.; Leimgruber, S.; Kargl, R.; Spirk, S.; Stana-Kleinschek, K.; Ribitsch, V. Creating Water Vapor Barrier Coatings from Hydrophilic Components. *ACS Appl. Mater. Interfaces* **2012**, *4*, 3199−3206.
(37) Spence, K. L.; Venditti, R. A.; Rojas, O. J.; Pawlak, J. J.; Hubbe, M. A. Water Vapor Barrier Properties of Coated and Filled Microfibrillated Cellulose Composite Films. *Bioresources* **2011**, *6*, 4370−4388.
(38) Ummartyotin, S.; Juntaro, J.; Sain, M.; Manuspiya, H. Development of Transparent Bacterial Cellulose Nanocomposite Film as Substrate for Flexible Organic Light Emitting Diode (OLED) Display. *Ind. Crops Prod.* **2012**, *35*, 92−97.
(39) Spence, K. L.; Venditti, R. A.; Habibi, Y.; Rojas, O. J.; Pawlak, J. J. The effect of chemical Composition on Microfibrillar Cellulose Films from Wood Pulps: Mechanical Processing and Physical Properties. *Bioresour. Technol.* **2010**, *101*, 5961−5968.
(40) Meier, M. M.; Kanis, L. A.; de Lima, J. C.; Pires, A. T. N.; Soldi, V. Poly(caprolactone triol) as Plasticizer Agent for Cellulose Acetate Films: Influence of the Preparation Procedure and Plasticizer Content on the Physico-chemical Properties. *Polym. Adv. Technol.* **2004**, *15*, 593−600.